

A spectral description for extreme sea states offshore Denmark: Part II Directional spreading function

Kevin Ewans¹, Hans Hansen², and Allan Zeeberg³

¹*MetOcean Research Ltd, New Plymouth, New Zealand.*

²*DHI A/S, Hørsholm, Denmark. Now HAW MetOcean ApS, Copenhagen, Denmark*

³*Total E&P Denmark A/S, Esbjerg, Denmark.*

Abstract

Power spectral density and frequency-dependent directional spreading functions that describe extreme sea states are required for TEPDK's Abnormal Wave Assessment and Risk Evaluation (AWARE) project. The spectral functions are needed for modelling extreme sea states realised in Monte Carlo simulations drawn from a statistical model of extreme conditions for the project. The input to the spectral models are the significant wave height, the spectral peak period, the spectral second-moment period, and the circular root-mean-square spreading at the spectral peak frequency – parameters that will be simulated from the statistical model.

The new spectral functions were developed from measurements of large sea states made with Directional Waverider buoys at TEPDK's locations, in the Danish Sector of the North Sea. This paper describes the new directional spreading function; a companion paper describes the new power spectral density function.

The new directional spreading function is based on a simple parameterisation of measured frequency-dependent spreading derived from the Directional Waverider buoys. It is defined in terms of the peak period and significant wave height, with different expressions depending on whether the dominant component in the spectrum is a wind-sea or a swell. A form for a combined wind-sea and swell sea state is also defined. The new spreading function is compared against measurements for the location.

1 Introduction

The AWARE project requires the specification of a spectrum (power spectral density function and frequency-dependent directional spreading function) for use in Monte Carlo simulations of the wave field in a large number of sea states representing the wave climate in the Danish sector of the North Sea. The primary focus of the AWARE project was extreme conditions, so the spectral model developed was optimised from the larger sea states in the wave measurements in the region.

The work reported in this paper established a description for the frequency-dependent wave directional spreading for large sea states. As the AWARE statistical model provides the spreading at the spectral peak as one of the sea state parameters produced in the simulations, the directional spreading model needed to be expressed in terms of the spreading at the spectral peak frequency. The specific spreading parameter is the circular root-mean-square spreading in degrees, often denoted by the Greek character σ . At a given frequency, the circular root-mean-square spreading is

an estimate of the directional width about the mean wave direction, in which a large proportion of the wave energy is propagating.

A description of the wave measurements and analysis is given in Section 2; general observations of the directional spreading is given in Section 3; the new spreading model is described in Section 4; and conclusions are given in Section 5.

2 Wave Measurements & Analysis

Directional wave measurements made with Datawell Directional Waverider (DWR) buoys were available at two relatively close locations in the Danish Sector of the North Sea. The locations are referred to as Location 2 (LOC2) and Location 4 (LOC4) and are shown in Figure 1. The Location 2 is 15 km Southeast of the Location 4.

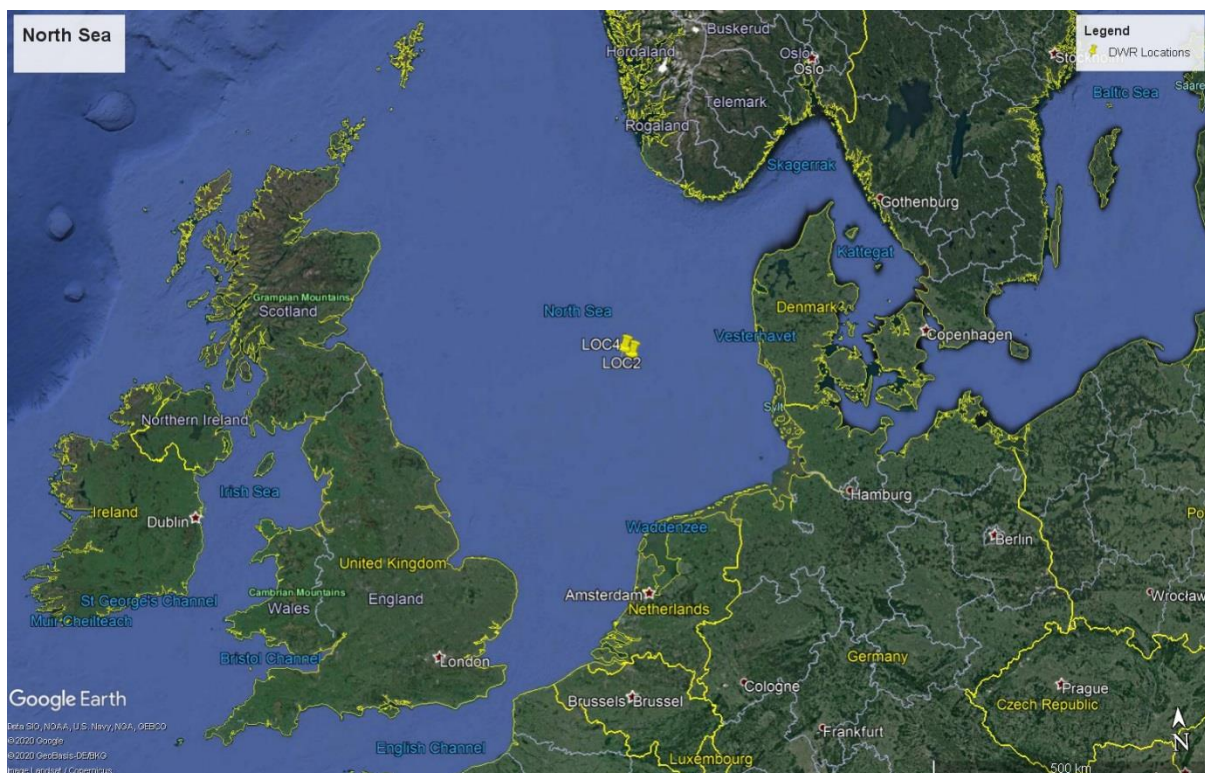


Figure 1 The LOC4 and LOC2 locations, indicated by marker pins, in the Danish Sector of the North Sea.

The details of the measurements are given in Table 1.

The LOC2 data were recorded over the period 17-Jan-2014 to 16-Jul-2016. The raw data for LOC2 consisted of two batches. The first, for the period 17-Jan-2014 to 15-Sep-2015, consisted of daily files of 1.28 Hz-sampled values of Heave, North, and West buoy displacements. Frequency spectra of hourly blocks of these data were calculated, following Welch (1967). Accordingly, frequency spectra consisting of 129 spectral estimates with a spectral resolution of 7.81×10^{-3} Hz over the range 0 Hz to 0.640 Hz were produced. Spectral estimates below 0.035 Hz and above 0.600 Hz were discarded, leaving 114 values. Frequencies below 0.035 Hz were outside of the Datawell-recommended operating range of the buoy, and frequencies above 0.600 Hz were sometimes found to contain spurious values.

The second batch of raw LOC2 data, for the period 16-Sep-15 to 16-Jul-2016, consisted of half-hourly files of 1.28 Hz-sampled values of Heave, North, and West buoy displacements. These were processed in the same way as the first batch, except that the resulting spectra represented 30-minutes of data, rather than 60-minutes as was the case for the first batch.

Parameters were computed from the power spectra for each of the vertical displacement signals, and an inspection of the significant wave height, H_{m0} , derived from the zeroth-moment of the spectrum, was made for each, to identify unrealistic values, corresponding to spikes or drop-outs. This resulted in a number of spectra being discarded.

In addition to the power spectra, frequency spectra of the mean direction and circular rms spreading were computed, from the first and second Fourier coefficients of the directional distribution, following Kuik *et al.* (1988).

Table 1 Measured Directional Wave Data

Location Name	Location Short Name	Water depth [m re. MSL]	Number of Records	H_{m0} Range [m]	T_p Range [s]
Location 2	LOC2	42	26,274	[0.03, 8.69]	[2.11, 23.4]
Location 4	LOC4	41	8,722	[0.57, 8.86]	[3.19, 18.4]

3 Observations

Scatter plots of H_{m0} against the second-moment period, T_{02} , derived from the zeroth and second moments of the power spectrum, H_{m0} against θ_p (the mean wave direction at the spectral peak), and σ_p (the circular rms spreading at the spectral peak, Kuik *et al.*, 1988) against θ_p are given in Figure 2. The data for the LOC2 location are plotted as blue dots, while those for the LOC4 location are plotted as brown dots. With consideration to the fact that there are three times more data at LOC2 than LOC4, the data for the two locations show similar features.

Curves corresponding to significant wave steepness, defined by $s_{02} = 2\pi H_{m0}/gT_{02}^2$, for s_{02} ratios of 1:14 and 1:19.7 are included in the H_{m0} against T_{02} plot. The steepness value of 1:19.7 corresponds to that of the Pierson-Moskowitz spectrum. Most of the points in the plot lie between the two wave steepness curves, indicating that most sea states are dominated by wind-sea waves. There are far fewer points with relatively low steepness; the sea states associated with these points are dominated by swell.

The clustering of the points in the scatter plots of H_{m0} against θ_p is consistent with the directions with long fetch corridors. The plots also show that the largest sea states are from the northwest, the corridor to the northern part of the North Sea. Most of the sea states from the northwest also have relatively low spreading. Sea states from northeast, the direction towards the Skagerrak coast are also associated with generally low spreading, probably because of the narrow fetch, which is constrained by the northern coast of Denmark and the southeast coast of Norway. The sea states from the northeast, which are also most probably wind-sea dominated can be relatively large.

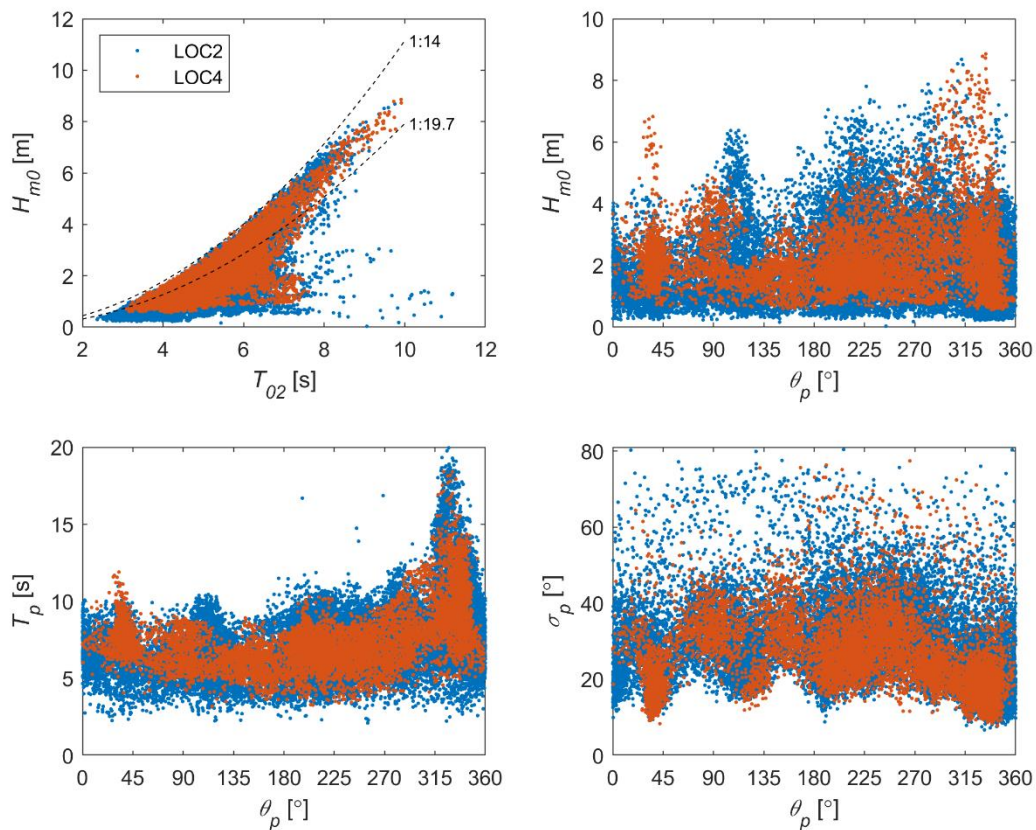


Figure 2 Scatter plots of H_{m0} against T_{02} , H_{m0} against θ_p (the mean wave direction at the spectral peak), and σ_p (the circular rms spreading at the spectral peak) against θ_p , for the LOC2 measurements (blue) and LOC4 measurements (brown).

Figure 3 shows measured circular rms spreading spectra, for the LOC2 and LOC4 data sets combined, for cases when wind-sea is the Primary component in the Torsethaugen spectral model (Ewans *et al.*, 2019). The spectra are binned according to the direction of the spectral peak wave direction of the sea states, and only those sea states with significant wave heights above the 99th percentile for the given directional sector are plotted. The abscissa is normalised frequency, f/f_p . Lines of the running mean (black) and the Ewans (1998) wind-sea spreading function (blue) are given for comparison.

The first observation to note in Figure 3 is the similarity of the shapes of the measured spectra when plotted by normalised frequency. This effect in wind-sea sea states is well known.

Secondly, the variation with mean wave direction is small. Comparison with the Ewans spectrum suggests some possible variations with the rate of increase of the spreading below and above the spectral peak frequency. For example, the increase for the northerly sectors above the spectral peak frequency matches the Ewans spectrum well, but the increase is faster than the Ewans spectrum for the other directional sectors. Similarly, the rate of increase for frequencies below the spectral peak frequency is similar to the Ewans spectrum for the southerly sectors but slower for the others. In addition, there is evidence that the spreading at the spectral peak frequency for the northwest and north sectors may be lower than that in the Ewans spectrum, perhaps indicating contribution from swell. Nevertheless, it appears that a single spreading function may be adequate for all directions.

The final observation to note is that the measured spectra clearly reach a plateau at both low and high frequencies, somewhat lower than the Ewans spectrum, which is based on measurements for which $f/f_p \lesssim 4.5$.

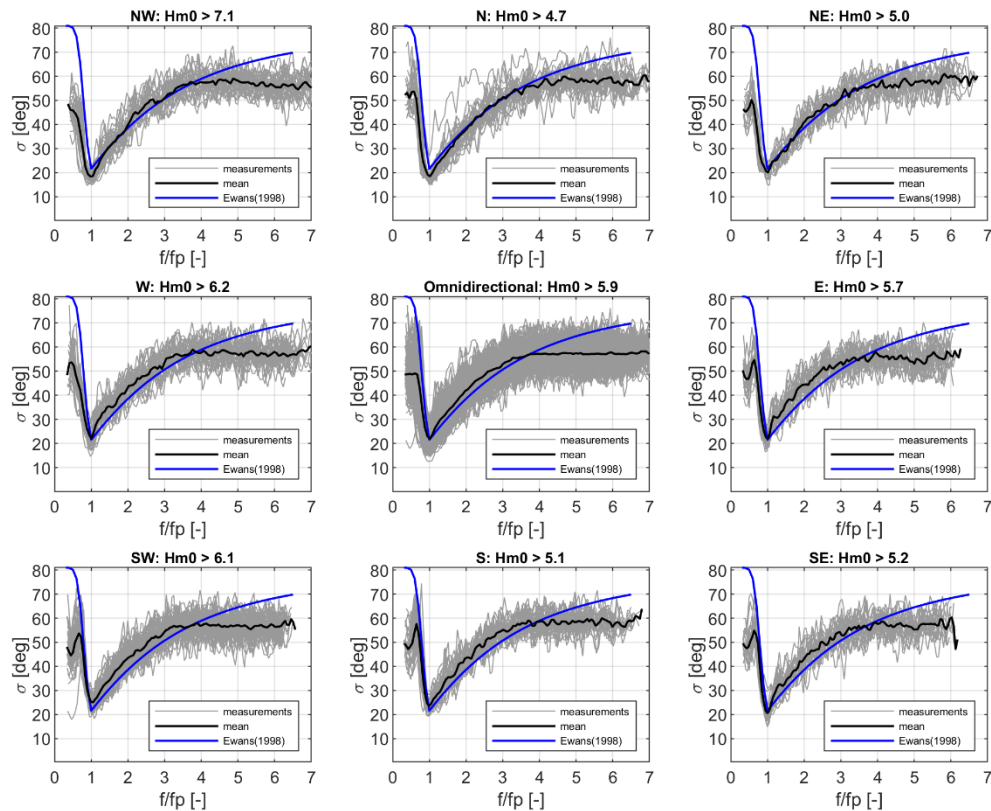


Figure 3 Circular rms spreading against normalised frequency for the sea states for which wind-sea is the Primary component and which exceed the specified threshold for the specified mean wave directions, for the combined LOC2 and LOC4 data sets. The black line is the running mean of the spectra, and the blue line is the Ewans (1998) spreading function.

The comparable plots for the cases when swell is the Primary component are given in Figure 4. Most sea states in this category are from the northerly sectors. The sectors that do not have large coastal fetches, such as the southeast, have few such sea states.

The main points to note regarding the spreading of these (swell-primary) sea states are:

1. The similarity of the spectra for the sectors that have many spectra, and their broad similarity with the shape of wind-sea spreading spectra for frequencies above the spectral peak frequency, likely due to substantial contribution of wind-seas at those frequencies.
2. The occurrence of spectra that have a rapid increase in spreading above the spectral peak frequency, similar to the rate observed below the spectral peak frequency.
3. The Ewans spreading function is less relevant for these sea states.

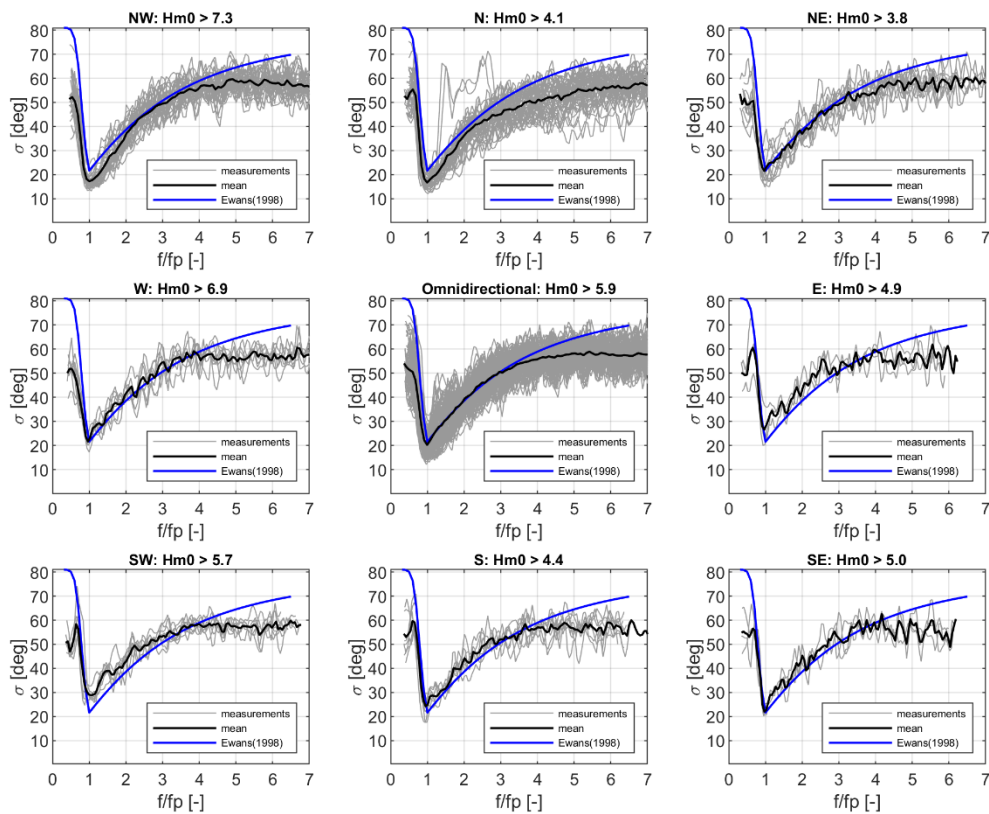


Figure 4 Circular rms spreading against normalised frequency for the seas states for which swell is the Primary component and which exceed the specified threshold for the specified mean wave directions, for the combined LOC2 and LOC4 data sets. The black line is the running mean of the spectra, and the blue line is the Ewans (1998) spreading function.

The intention in the Monte Carlo simulations is to set the mean wave direction for all frequencies in the spectrum to be equal to the peak wave direction. The voracity of the assumption that the mean direction is constant for all frequencies was evaluated by inspection of the spectra for sea states with $H_{m0} > 7$ m in the Location 2 combined data set, 32 in total. Three of the spectra, for 22-Oct-2014 02:00 hrs, 15-Jan-2015 23:00 hrs, and 8-Feb-2015 02:00 hrs, meeting this criterion are given in Figure 5, by way of example. The plots in the top row correspond to the mean wave direction (left axis) and power spectral density (right axis), and those in the bottom rows correspond to the circular rms spreading (left axis) and power spectral density (right axis). As can be seen in Figure 5, the mean directions at each frequency are essentially uniform across the spectrum, and this was the case for most of the 32 spectra. Low-frequency swell is visible in some spectra, and in these, a small difference in the direction of the swell component from the wind-sea component was apparent. All such cases corresponded to a westerly wind-sea and a northwesterly swell. In all of the cases when a low-frequency swell was apparent, the spectral levels of the swell were more than an order of magnitude lower than the wind-sea, and in some cases swamped by the wind-sea component. Thus, the accompanying swell is virtually insignificant by comparison with the wind-sea event, and the assumption of constant wave direction with frequency would appear reasonable for the application.

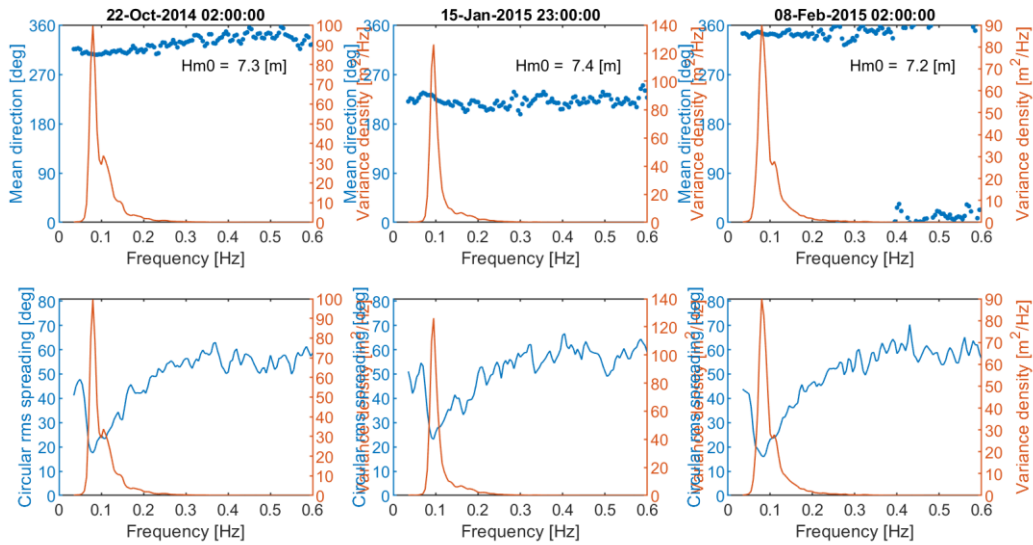


Figure 5 Frequency spectra for 22-Oct-2014 02:00 hrs, 15-Jan-2015 23:00 hrs, and 8-Feb-2015 02:00 hrs, for the Location 2 data set. Top row: mean direction (left axis) and power spectrum (right axis), Bottom row: circular rms spreading (left axis) and power spectrum (right axis).

4 The AWARE Spreading Model

4.1 Spreading Characteristics Considered in the Model

The spectra of individual sea states suggests the existence of an upper limit at both low and high frequencies at which the spreading plateaus. To investigate this further, the spreading spectra for sea states exceeding specific H_{m0} thresholds were computed, for the combined LOC2 and LOC4 data sets. These are plotted in Figure 6. The upper plot gives the results for the sea states in which swell is the Primary component; the lower plot gives the curves for the sea states in which wind-sea is the Primary component. The curve for $H_{m0} > 5$ is over-plotted in bold black for emphasis.

In the case when swell is the Primary component, the high-frequency plateau appears to be a function of the H_{m0} , increasing with increasing threshold until the threshold $H_{m0} > 5$ m, at which point the plateau is around 57° . The curves appear to reach a plateau by $f/f_p = 5$.

A similar but opposite effect appears to occur for the low-frequency plateau. In this case, the plateau decreases with increasing H_{m0} threshold until the threshold $H_{m0} > 5$ m, at which point the plateau is around 53° .

In the case when the wind-sea is the Primary component, the high-frequency plateau is also around 57° and is reached by all the curves by $f/f_p = 5$. The curves indicate that the value of f/f_p at which the plateau is reached decreases with increasing threshold, until the threshold $f/f_p = 5$ m, at which point this effect ceases.

As for the swell case, low-frequency plateau appears to decrease with increasing H_{m0} , but unlike the swell case, the wind-sea case continues to decrease for thresholds above the $H_{m0} > 5$ m threshold.

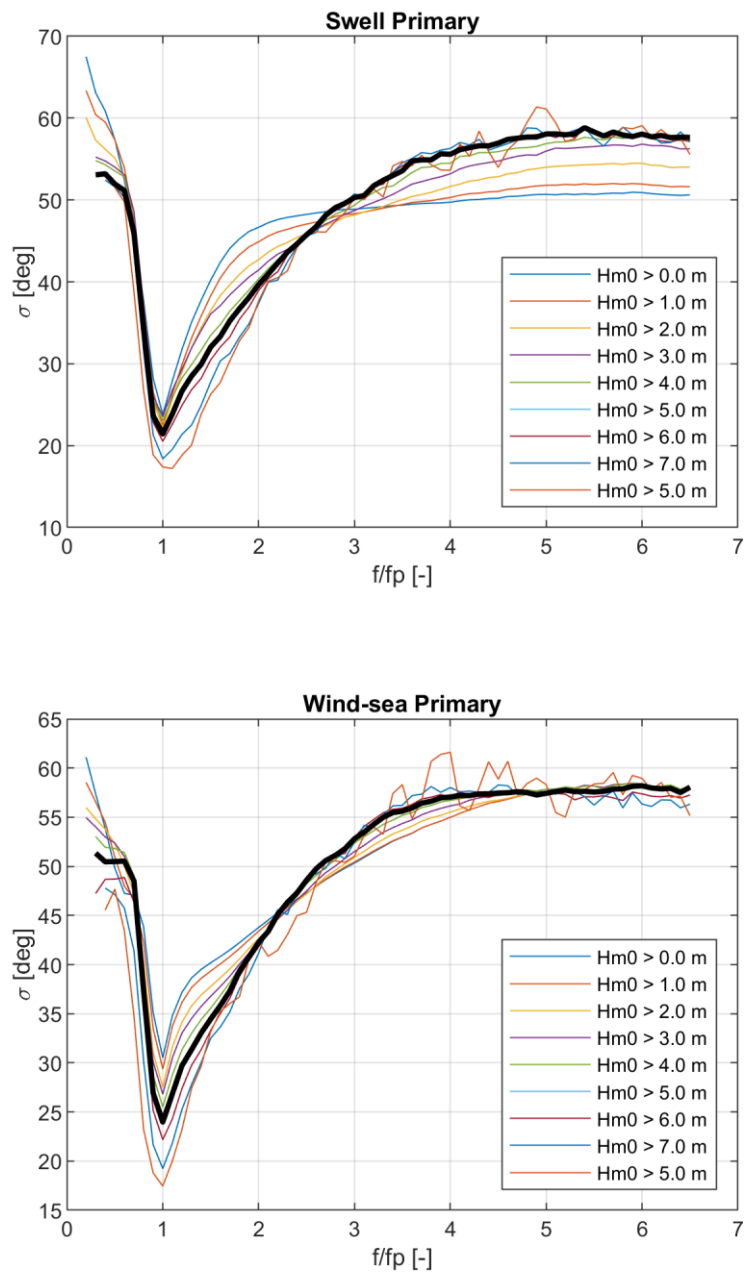


Figure 6 Curves for the mean spreading of sea states exceeding the specified H_{m0} threshold, for the combined LOC2 and LOC4 data sets. Upper plot gives the results for the sea states in which swell is the Primary component. The lower plot gives the curves for the sea states in which wind-sea is the Primary component. The curve for $H_{m0} > 5$ m is over-plotted in bold black for emphasis.

To provide additional resolution on the effects of H_{m0} on the spreading spectrum characteristics, mean spreading spectra were computed for one-metre bins of H_{m0} . The results are plotted in Figure 7. The effects seen in Figure 6 are somewhat clearer in Figure 7. In the case of swell being the Primary component (top plot), the bins for $H_{m0} > 5$ m appear to converge (and plateau) for $f/f_p \approx 0.6$, and $f/f_p \approx 5$. In the case of wind-sea being the Primary component, the plots suggest the

means tend to plateau at successively lower values of H_{m0} , and at successively lower values of f/f_p with increasing H_{m0} , and the means for the bins for $H_{m0} > 5$ m appear to converge (and plateau) for $f/f_p \approx 4$.

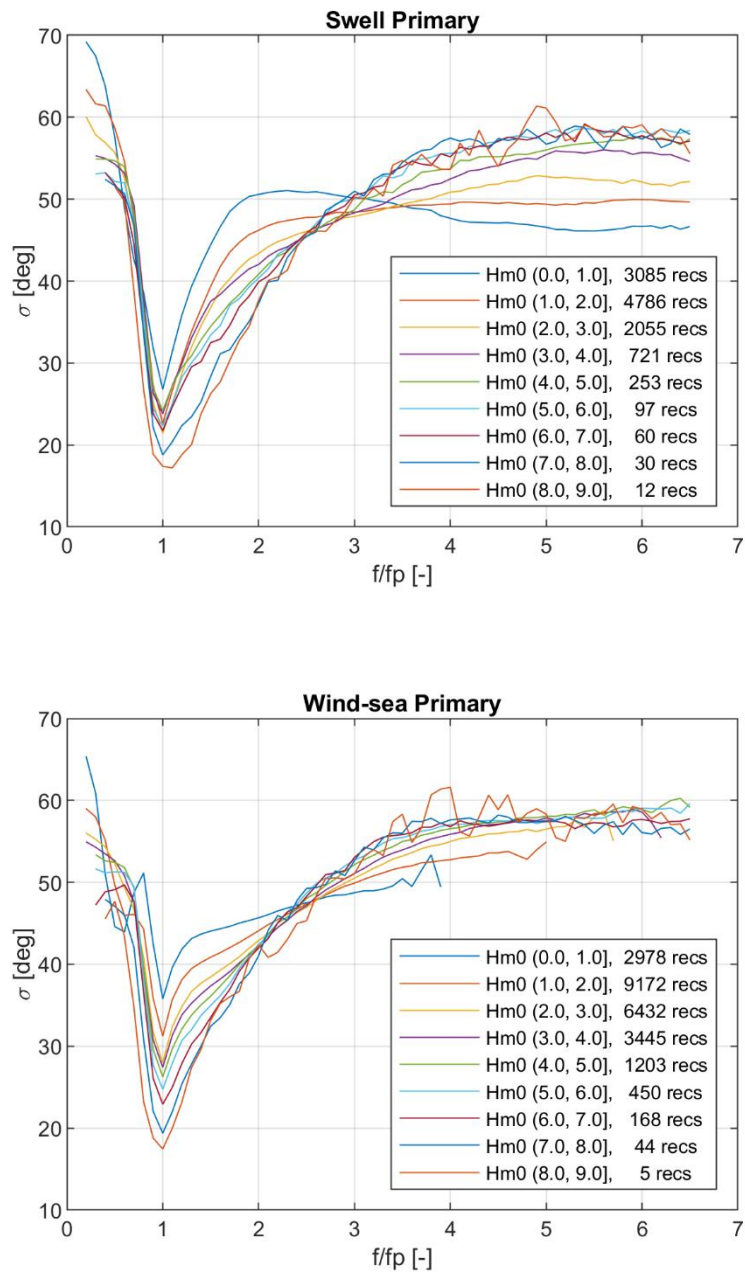


Figure 7 Curves for the mean spreading of sea states for the specified H_{m0} bins, for the combined LOC2 and LOC4 data sets. Upper plot gives the results for the sea states in which swell is the Primary component. The lower plot gives the curves for the sea states in which wind-sea is the Primary component.

The plots of mean rms spreading against H_{m0} bin, for the specified values of f/f_p in Figure 8, provide another perspective. The cases when swell is the Primary component are in the top plots

($f/f_p \leq 1$ – left, $f/f_p \geq 1$ – right) and the cases when wind-sea is the Primary component are in the bottom plots. The top left plot indicates that the mean spreading decreases slowly with increasing H_{m0} but a mean spreading of around 53° appears to be a maximum for $f/f_p < 0.6$ at larger seas states. The top right plot shows that the mean spreading decreases slightly with increasing H_{m0} for $f/f_p = 1$ and $f/f_p = 2$, but is more or less steady for higher values of f/f_p and it reaches a maximum of around 58° for $f/f_p > 5$.

The bottom left plot shows the mean spreading for $f/f_p = 0.8, 0.9, 1.0$ steadily decreases with increasing H_{m0} , but reaches a maximum that depends on H_{m0} for $f/f_p < 0.6$. The bottom right plot shows the mean spreading at $f/f_p = 1$ steadily decreases with increasing H_{m0} , but appears to reach a maximum of around 57° for $f/f_p > 4$.

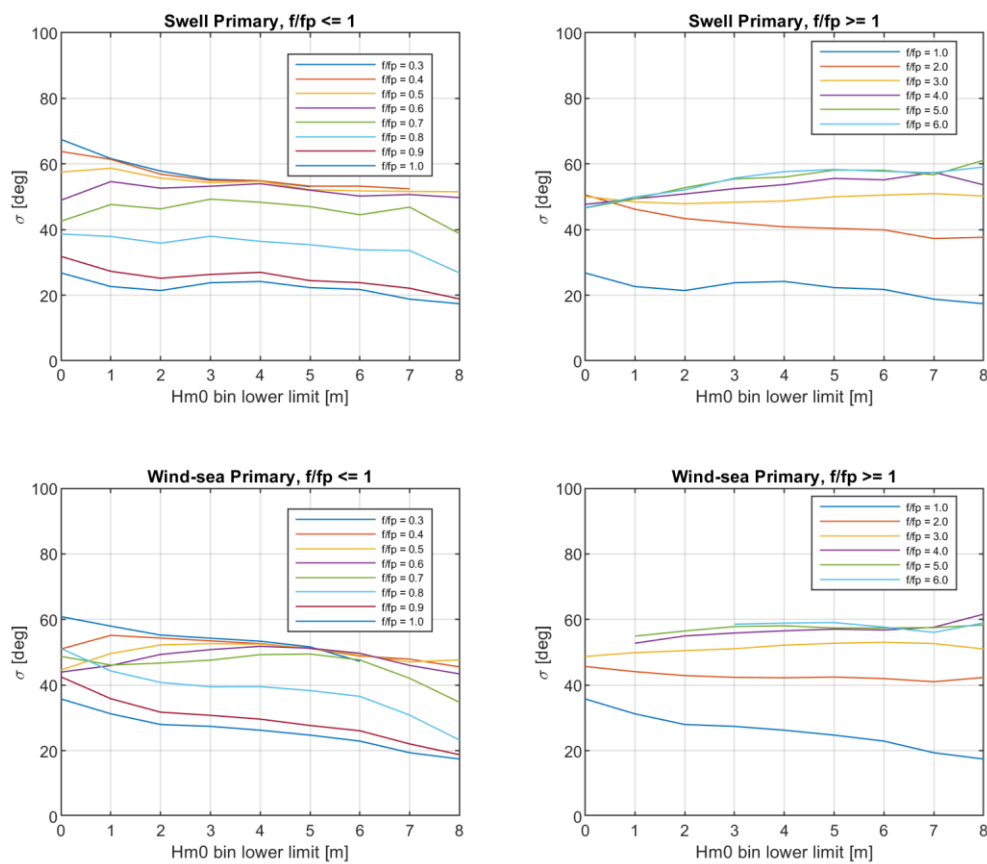


Figure 8 Plots of mean rms spreading against H_{m0} bin, for the specified values of f/f_p , for the combined LOC2 and LOC4 data sets – swell Primary (upper plots), wind-sea Primary (lower plots).

4.2 Model Description

AWARE Swell Model

For $\frac{f}{f_p} < 1$, the model is based on a function of the form $\sigma = \sigma_p + a_{sw} \left(1 - \frac{f}{f_p}\right)^{1.4}$ that equals 52.3° for $\frac{f}{f_p} \leq 0.6$ and equals σ_p for $\frac{f}{f_p} = 1$, which allows a_{sw} to be determined.

For $\frac{f}{f_p} \geq 1$, the model is based on a function of the form $\sigma = \left(b_{sw} + c_{sw} \left(\frac{f}{f_p} \right)^{-2} \right)^{-1}$ that equals σ_p for $\frac{f}{f_p} = 1$ and equals 58.0° for $\frac{f}{f_p} > 5$, which allows b_{sw} and c_{sw} to be determined.

The values of 52.3° and 58.0° correspond to the averages over the respective frequency bands of the DWR spreading spectra for the combined LOC2 and LOC4 data sets, for $H_{m0} > 5$ m, and the respective functions were selected following trials with several candidate functions.

Accordingly, the AWARE swell model for circular rms spreading, σ_{Wsw} , is given by

$$\sigma_{Wsw}(f; \sigma_p) = \begin{cases} 52.3^\circ & \text{for } \frac{f}{f_p} \leq 0.6 \\ \sigma_p + \frac{(52.3 - \sigma_p)}{0.4^{1.4}} \left(1 - \frac{f}{f_p} \right)^{1.4} & \text{for } 0.6 < \frac{f}{f_p} \leq 1 \\ \frac{1}{b_{sw} + c_{sw} \left(\frac{f}{f_p} \right)^{-2}} & \text{for } 1 < \frac{f}{f_p} \leq 5 \\ 58.0^\circ & \text{for } 5 < \frac{f}{f_p} \end{cases} \quad (1)$$

where

$$b_{sw} = \frac{25}{24(58.0)} - \frac{1}{24\sigma_p} \quad (2)$$

and

$$c_{sw} = \frac{25}{24} \left(\frac{1}{\sigma_p} - \frac{1}{58.0} \right) \quad (3)$$

AWARE Wind-sea Model

For $\frac{f}{f_p} < 1$, the model is based on a function of the form $\sigma = \sigma_p + a_{ws} \left(1 - \frac{f}{f_p} \right)^{1.5}$ that equals σ_{LF} for $\frac{f}{f_p} \leq \frac{f}{f_{pLF}}$ and equals σ_p for $\frac{f}{f_p} = 1$, which allows a_{ws} to be determined.

For $\frac{f}{f_p} \geq 1$, the model is based on a function of the form $\sigma = \left(b_{ws} + c_{ws} \exp\left(-\frac{f}{f_p}\right) \right)^2$ that equals σ_p for $\frac{f}{f_p} = 1$ and equals 57.6° for $\frac{f}{f_p} > 4$, which allows b_{ws} and c_{ws} to be determined.

The values of σ_{LF} and $\frac{f}{f_{pLF}}$ were derived from averages of the DWR spreading spectra for the combined LOC2 and LOC4 data sets, over H_{m0} binned in 1 m intervals.

The value of 57.6° corresponds to the average of DWR spectra for the combined LOC2 and LOC4 sites, for $H_{m0} > 5$ m.

Accordingly, the AWARE wind-sea model for circular rms spreading, σ_{Wws} , is given by

$$\sigma_{Wws}(f; \sigma_p, H_{m0}) = \begin{cases} \sigma_{LF} & \text{for } \frac{f}{f_p} \leq \frac{f}{f_{p_{LF}}} \\ \sigma_p + \frac{(\sigma_{LF} - \sigma_p)}{\left(1 - \frac{f}{f_{p_{LF}}}\right)^{1.5}} \left(1 - \frac{f}{f_p}\right)^{1.5} & \text{for } \frac{f}{f_{p_{LF}}} < \frac{f}{f_p} \leq 1 \\ \left(b_{ws} + c_{ws} \exp\left(-\frac{f}{f_p}\right)\right)^2 & \text{for } 1 < \frac{f}{f_p} \leq 4 \\ 57.6^\circ & \text{for } 4 < \frac{f}{f_p} \end{cases} \quad (4)$$

where

$$\begin{aligned} \frac{f}{f_{p_{LF}}} &= 0.4 & \text{for } & H_{m0} \leq 4.429 \\ \frac{f}{f_{p_{LF}}} &= -0.07H_{m0} + 1.11 & \text{for } & 4.429 \leq H_{m0} \leq 10.14 \\ \frac{f}{f_{p_{LF}}} &= 0.8 & \text{for } & H_{m0} \geq 10.14 \end{aligned} \quad (5)$$

and

$$\begin{aligned} \sigma_{LF} &= \frac{1}{2} 1.0^2 - 8.44(1.0) + 82.2 \approx 74.3^\circ & \text{for } & H_{m0} < 1.0 \\ \sigma_{LF} &= \frac{1}{2} H_{m0}^2 - 8.44H_{m0} + 82.2 & \text{for } & 1.0 \leq H_{m0} \leq 8.4 \\ \sigma_{LF} &= \frac{1}{2} 8.4^2 - 8.44(8.4) + 82.2 \approx 46.6^\circ & \text{for } & H_{m0} > 8.4 \end{aligned} \quad (6)$$

and

$$c_{ws} = \frac{\sigma_p^{0.5} - 57.6^{0.5}}{\exp(-1) - \exp(-4)} \quad (7)$$

and

$$b_{ws} = \sigma_p^{0.5} - c_{ws} \exp(-1) \quad (8)$$

AWARE Model

When wind-sea is the Primary component, the AWARE model for circular rms spreading, $\sigma_W(f)$, is given Equations (4) to (8).

When swell is the Primary component, the AWARE model for circular rms spreading, $\sigma_W(f)$, is given by

$$\sigma_W(f) = \frac{\sigma_{Wsw}(f; \sigma_p, H_{m0})G_{sw}(f) + \sigma_{Wws}(f; \sigma'_p)G_{ws}(f)}{G(f)} \quad (9)$$

where

$$\sigma'_p = 2.17\sigma_p \quad (10)$$

The value of 2.17 corresponds to the 50 percentile of the ratio of the rms spreading at the spectral peak frequency of the wind-sea component to that at the spectral peak when swell is the Primary component, for sea states with $H_{m0} > 5$ m in the combined LOC2 and LOC4 data sets.

4.3 Model Evaluation

The AWARE spreading model is compared with frequency-normalised mean measured rms spreading for specified H_{m0} bins in Figure 9. The AWARE model is based on the mid-point H_{m0} of each bin. The agreement is very good, but there is an apparent small over-estimation at frequencies above the spectral peak frequencies, for some of the bins.

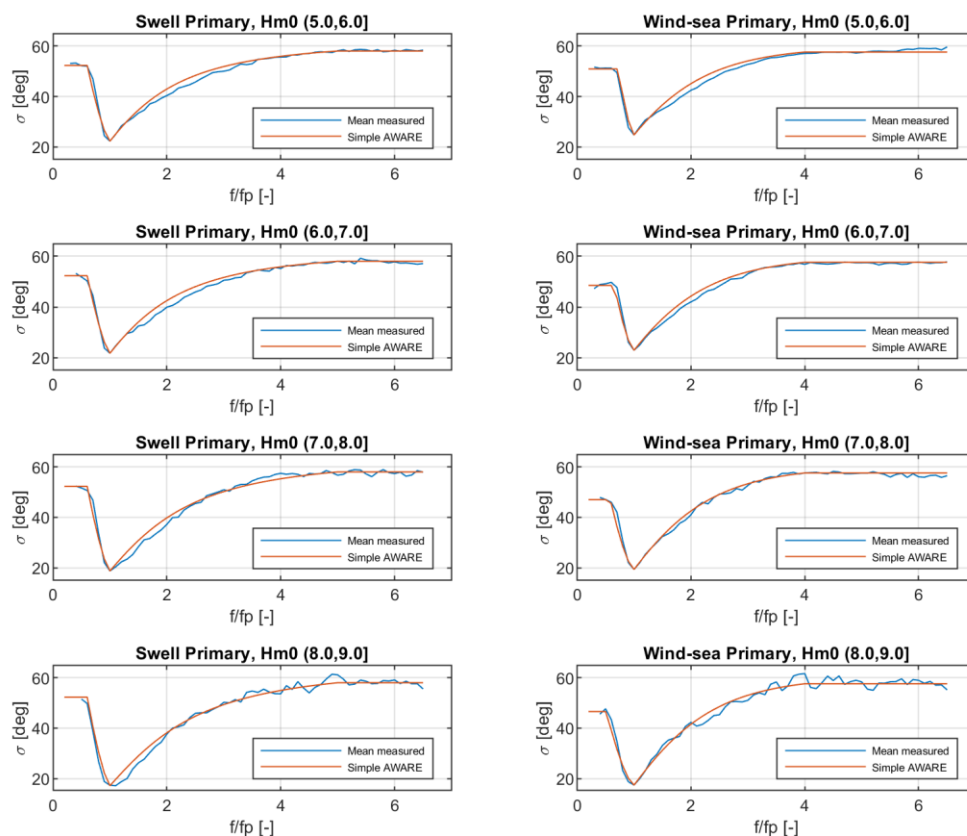


Figure 9 Frequency-normalised mean measured rms spreading for the specified H_{m0} bins, together with the AWARE model, based on the mid-point H_{m0} of each bin.

Comparisons are also made for specific sea states - comparisons of the three largest sea states in the combined LOC2 and LOC4 data sets are given in Figure 10. Plots of the power, mean direction, and circular rms spreading spectra are given. The AWARE model spectrum, and the swell (AWAREsw) and wind-sea (AWAREws) spectra that make up the AWARE model spectrum are plotted with the measured power spectrum. The spreading function described in Section 4.2 is plotted with the measured spreading. The mean sigma values given in the spreading plots are determined from the spectral-density-weighted sigma values.

The plots show the model spreading does well in predicting the measured spreading for all three cases, but particularly for the case when wind-sea is the Primary component (0731 hrs). The

relatively large breadth of the trough in the spreading around the spectral peak for all three cases is indicative of the presence of both a wind-sea and swell component with similar peak frequencies, both apparently arriving from the northwest. In this case a model involving a wind-sea and swell would appear appropriate, but the relative levels and peak frequencies of the respective components resulting from the model are not consistent with this.

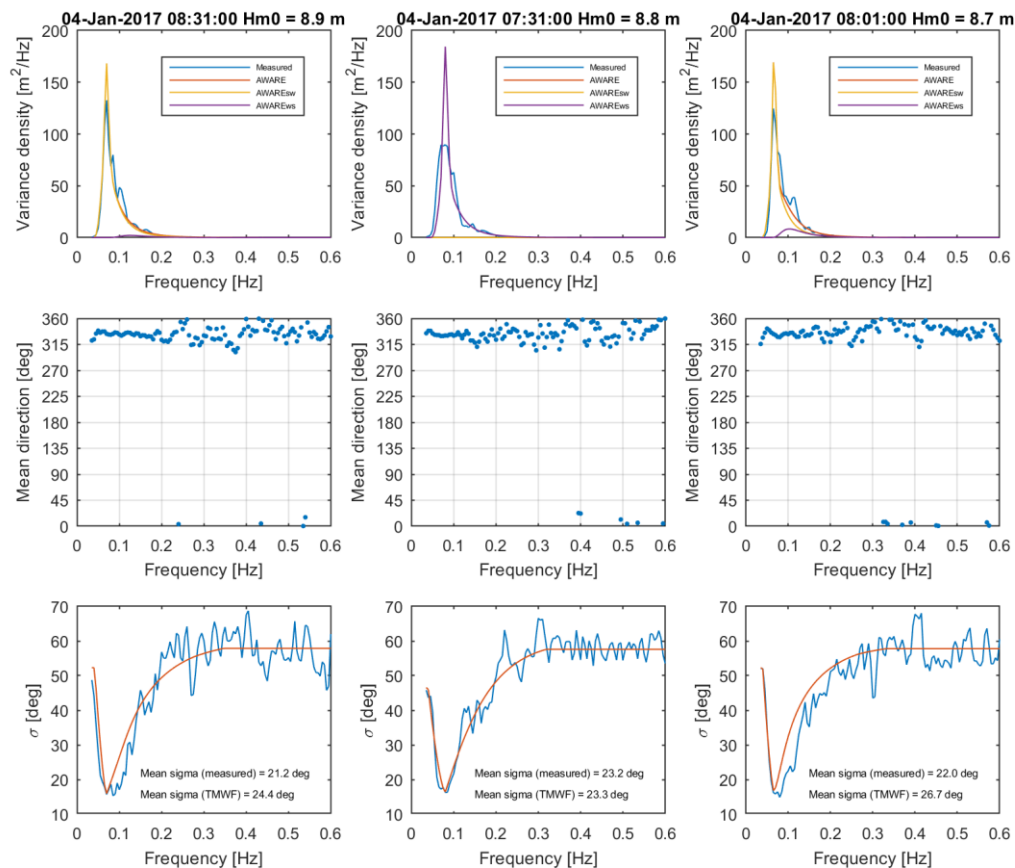


Figure 10 Power (top), mean direction (middle), and circular rms spreading spectra (bottom) for the largest three sea states in the combined LOC2 and LOC4 data sets. The AWARE model spectrum, and the swell (AWAREsw) and wind-sea (AWAREws) spectra that make up the AWARE model spectrum are plotted with the measured power spectrum. The AWARE spreading function described in Section 4 is plotted with the measured spreading. Swell is the Primary component for the spectra recorded at 0831 and 0801 on 4-Jan-17 (left and right plots), and wind-sea is the Primary component for the spectra recorded at 0731 (middle plots). The mean sigma values are determined from the spectral-density-weighted sigma values.

An overall comparison of the model spreading against measurements is given in Figure 11, which gives scatter plots of the mean circular rms spreading estimated for each sea state in the combined LOC2 and LOC4 data base. Plots are given for each of eight directional sectors, with sea states with significant wave height greater than 5 m coloured brown and those of these in which swell is the primary component ($T_{pf} > T_p$) coloured gold. The agreement is good for the sea states with $H_{m0} > 5$ m, with little difference between the Swell Primary and Wind-sea Primary sea states and with direction. There is more spread in the lower sea states, particular for the Northerly sectors. A number of these were inspected and found to be due to sea states involving multiple peaks.

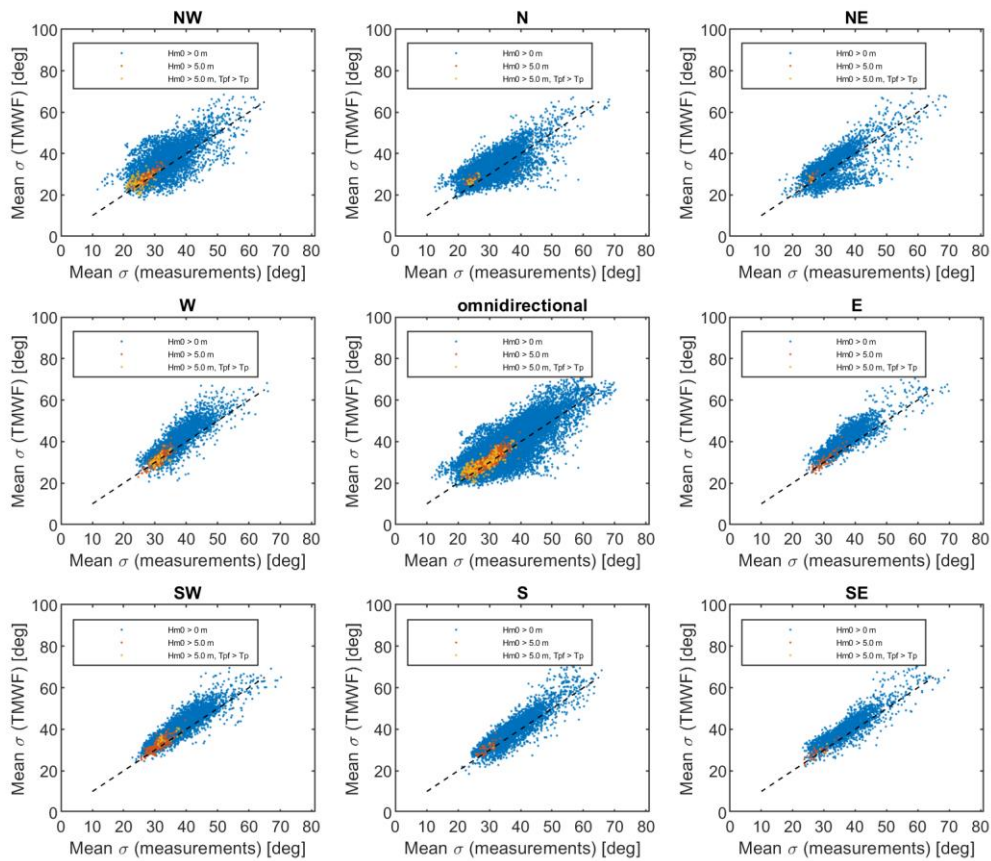


Figure 11 Scatter plots of the AWARE model (AWARE) mean circular rms spreading against the measured values for the combined LOC2 and LOC4 data sets, for each directional sector and the omnidirectional case. Points corresponding to sea states for which $H_{m0} > 5$ m are coloured brown, and those sea states above this threshold for which swell is the Primary component in the Torsethaugen description ($T_{pf} > T_p$) are coloured gold

6 Conclusions

High quality Directional Waverider Data recorded at the Location 2 and Location 4 locations in the Danish sector of the North Sea, have allowed a new model for the frequency-dependent circular rms spreading to be developed, for application in structural reliability studies. Overall, the new model has good skill, particularly for sea states with significant wave height greater than five metres.

Acknowledgements

We thank Total for permission to publish this work.

References

Evans, K. C., 1998. Observations of the directional spectrum of fetch-limited waves. *Journal of Physical Oceanography*, 28, pp. 495–512.

- Ewans, K.C., Hansen, H, and A. Zeeberg, 2019. A spectral description for extreme sea states offshore Denmark - Part I: Power Spectrum. *2nd International Workshop on Waves, Storm Surges and Coastal Hazards*, Melbourne, 10th – 15th November 2019.
- Kuik, A.J., G. Ph. van Vleddar, and L.H. Holthuisen, 1988. A method for the routine analysis of pitch-and-roll buoy wave data. *J. Phys. Oceanogr.*, **18**, 1020-1034.
- Welch, P.D., 1967. The use of the fast Fourier transform for the estimation of the power spectra: a method based on time averaging over short, modified periodograms. *IEEE Transactions of audio electroacoustics* AU-15; 70-75.